Front. Optoelectron. China 2010, 3(3): 228–231
DOI 10.1007/s12200-010-0113-x

RESEARCH ARTICLE

Bis-(8-hydroxyquinoline) mercury nanoribbons: preparation, characterization and photoconductivity

Li LIU[1,2], Mingwang SHAO (✉)[1,3], Xiuhua WANG[1]

1 Anhui Key Laboratory of Functional Molecular Solids, College of Chemistry and Materials Science, Anhui Normal University, Wuhu 241000, China
2 College of Biochemical Engineering, Anhui Polytechnic University, Wuhu 241000, China
3 Functional Nano and Soft Materials Laboratory, Soochow University, Suzhou 215123, China

© Higher Education Press and Springer-Verlag Berlin Heidelberg 2010

Abstract Bis-(8-hydroxyquinoline) mercury nanoribbons with average width of 300 nm, thickness of 50 nm and length of up to tens of micrometers were synthesized by a facile solvothermal method. X-ray powder diffraction and Fourier transform infrared spectrum were employed to determine their structure. The conductivity of a bundle of nanoribbons was also measured, which exhibited linear current-voltage characteristics and excellent photoresponse to light, indicating their potential applications in photoswitch nano-devices in the future.

Keywords 8-hydroxyquinoline, nanoribbons, photoswitches

1 Introduction

In the past decades, the demands of technological development in electronics have aroused tremendous development of nanoscale electronic and optoelectronic devices based on functional nanomaterials [1,2]. Since the functional materials' crystallinity and molecular arrangement influence the performance of the devices greatly [3–5], nanomaterials with various morphologies have been widely studied. Among those, one-dimensional (1D) nanostructures particularly received high attentions in the past few years for their unique electronic and optic properties and prospective applications in nanometer-scale devices [6,7].

Nowadays, 1D organic nanomaterials have emerged as promising and prospective next-generation materials owing to their superior properties compared with 1D inorganic nanomaterials, such as variety, flexibility, multifunctionality, designability, and tailorability [8–10]. However, there are only a few successful preparations of 1D organic nanomaterials reported up to now, such as self-assembly methods [11,12], templates [13], and vapor deposition techniques [14].

Since the efficient low-voltage-driven organic light-emitting diodes based on tris-(8-hydroxyquinoline)aluminum (AlQ_3) were first reported in 1987 [15], 8-hydroxyquinoline complexes have attracted wide attentions as important organic semiconductor materials because of their wonderful physical and chemical properties, and broad applications in many fields [16–18]. Recently, Li et al. obtained AlQ_3 and CdQ_2 nanorods via a solution-based route with surfactant [19]. Zhu et al. synthesized ZnQ_2 by sonochemical route from the water/oil microemulsion [20].

In this work, a facile solvothermal method without the assistance of templates and the contamination from the surfactants was employed to prepare bis-(8-hydroxyquinoline)mercury (HgQ_2) nanoribbons. A photoconduction device was fabricated based on the nanoribbons, and the photoconductive property was measured. The current-voltage (*I-V*) characteristics of the as-prepared products exhibited good linear behavior with the fast and reversible photoswitching response under on/off light exposure conditions. This conclusion was interesting and might be found a potential application in nano-optoelectronic devices in the future.

2 Experiment

2.1 Materials

All the chemical reagents were of analytical grade and used without further purification.

Received October 31, 2009; accepted January 20, 2010

E-mail: mwshao@mail.ahnu.edu.cn

2.2 Preparation of HgQ_2 nanoribbons

In a typical synthesis, 0.5 mmol $HgCl_2$ and 1 mmol 8-hydroxyquinoline were dissolved into 40 mL methanol under stirring, which was transferred into a Teflon-lined autoclave of 60 mL capacity and heated to 140°C for 10 h and cooled to room temperature naturally. Then ultrapure water was added into the resulting solution dropwisely under violent stirring. The resulting suspension was separated centrifugally, washed with ultrapure water several times, and then dried under vacuum at 60°C for 12 h.

2.3 Characterization

The powder X-ray diffraction (XRD) pattern was recorded on a Shimadzu XRD-6000 X-ray diffractometer equipped with CuKα radiation ($\lambda = 0.15406$ nm); a scanning rate of 0.05°/s was applied to record the pattern in the 2θ range of 5°–60°. The morphology and size of the products were studied by a Hitachi S-4800 scanning electron microscope (SEM). Fourier transform infrared (FTIR) spectrum was obtained with KBr pellets for solids on a Shimadzu FTIR-8400S spectrometer. The electrical measurements were tracked with a CHI 620B electrochemical workstation. The low magnification image was taken from an Olympus optical microscope.

3 Results and discussion

The XRD pattern of the as-prepared HgQ_2 nanoribbons is shown in Fig. 1. The peaks at 2θ of 8.18°, 16.44°, 24.78°, 33.22° and 41.90° are strong. This pattern may be indexed as the hexagonal phase with crystal constants $a = 13.9331 \pm 0.0912$ nm, and $c = 10.7222 \pm 0.0928$ nm, using the Hesse-Lipson method [21,22]. The peaks of (00l) are strongest, which indicates that the growth direction of the as-prepared products is (001).

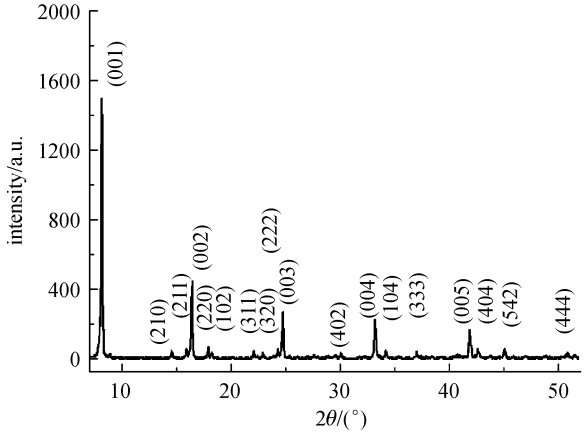


Fig. 1 XRD pattern of products

The FTIR spectrum is recorded to reveal the composition of HgQ_2, as shown in Fig. 2. The quinoline's characteristic stretching vibrations (1612–1458, 1303, 1379, 821, 756 cm^{-1}), aromatic amine resonances (C-N, 1234, 1265, 1373 cm^{-1}) and the C-O stretching vibration at 1099 cm^{-1} are clearly observed. The peak at 486 cm^{-1} is assigned to the Hg-N stretching vibration. The hydroxy peaks at 3306 and 1220 cm^{-1} disappear in the spectrum. All of the vibrations may be assigned to HgQ_2 [23], which further support that the as-prepared products are pure HgQ_2.

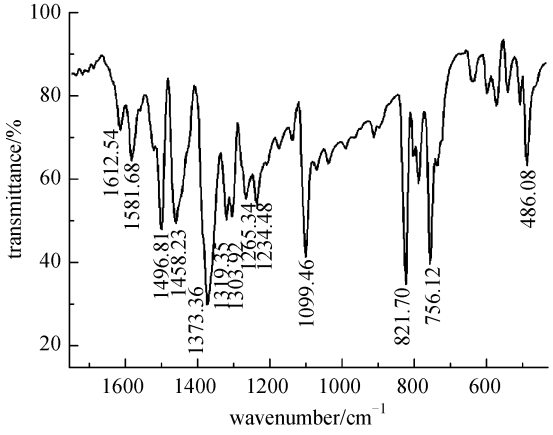
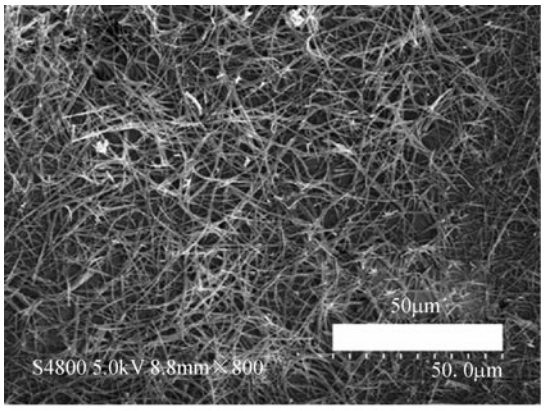


Fig. 2 FTIR spectrum of the products

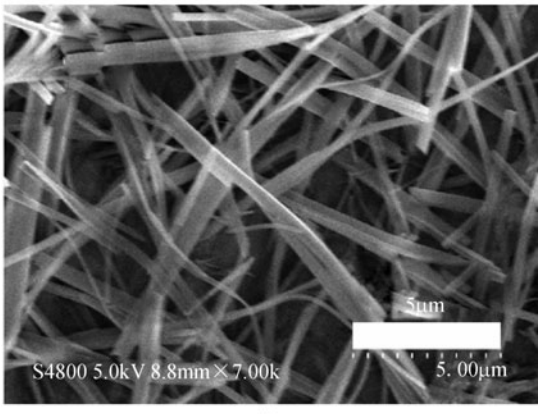
Figure 3(a) displays a panoramic SEM image of the as-prepared HgQ_2, which shows the ribbon-like morphology with lengths up to several hundreds of micrometers. The high magnification SEM image shown in Fig. 3(b) further reveals the ribbons with average width of 300 nm and thickness of 50 nm.

To measure the conductivity of the products, indium tin oxide (ITO) coated glass with the electrode gap of 25 μm was employed as the substrate. A bundle of HgQ_2 nanoribbons were dispersed and bridged over the electrodes with an effective length of about 40 μm, as shown in the inset of Fig. 4(a). To increase the injection of the device, gold gap electrodes were fabricated on the substrate by thermal evaporation with a micrometer-sized Au wire as the mask; by slightly moving the Au-wire mask, Au-Au gap electrodes were deposited [24]. Then the conductivity was measured in a dark box or under illuminated by using an incandescent lamp (12 V, 10 W). To decrease the thermal effect, the power of the incandescent lamp was only 10 W, and the distance of the device-to-light source was 10 cm.

Figure 4(a) shows the $I-V$ curves measured in dark and under illumination by using an incandescent lamp (12 V, 10 W) for comparison. Both of them exhibit good linear behavior, which proves a fine ohmic contact between the HgQ_2 nanoribbons and Au electrodes. The current of the

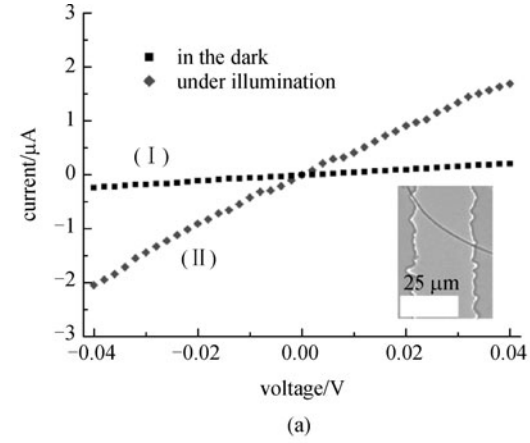


(a)

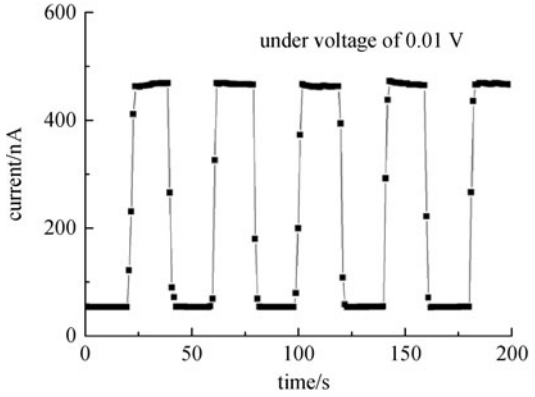


(b)

Fig. 3 SEM images of the products. (a) Low magnification; (b) high magnification



(a)



(b)

Fig. 4 Photoresponse of a bundle of products. (a) I–V curves in the dark or under illumination, and the image of the products between two Au electrodes from an optical microscope (inset); (b) photoresponse characteristics of the device during light switching on/off

nanoribbons rapidly increases under illuminating with an incandescent lamp. Figure 4(b) shows the reversible photoresponse characteristic of HgQ_2 during light switching on/off. A voltage of 0.01 V was applied across the two electrodes (Au-Au electrodes), and the current recorded during the light was alternately turned on and off at 20-s intervals. It is clearly observed that the conductivity of the HgQ_2 nanoribbons promptly increases or decreases according to the illumination on/off, which shows that the products have excellent photoresponse.

The photoswitch is attributed to the enhanced carrier density in the nanoribbons and the reduced depletion width. This behavior can be simply explained by the desorption of oxygen ions (O^-,O_2^- or O^{2-}) on the surface of the nanoribbons. Under illumination, the energy from the light excites the electrons in the semiconductor HgQ_2 jumping from the valence band into the conduction band, leaving holes in valence band, increasing the charge carrier concentration via direct electron-hole pair creation and, thus, enhancing the current of the nanoribbons. At the same time, oxygen ions capture the photoexcited holes, which liberates the oxygen species and leads to the increase of current attributed to both an enhanced carrier density in the nanoribbons and a narrower depletion width [25].

4 Conclusion

In summary, large-scale and high-purity HgQ_2 nanoribbons were successfully synthesized via a facile solvothermal approach, without the use of a template or a surfactant. The photocurrent of a bundle of HgQ_2 exhibited unique, fast and reversible photoswitching response. This work might have potential application in organic semiconductive or photosensitive nanodevices in the future.

Acknowledgements This work was supported by the National Natural Science Foundation of China (Grant No. 20571001) and Anhui Provincial Natural Science Foundation of Universities (No. KJ2009B003Z).

References

1. Chiu J J, Wang W S, Kei C C, Perng T P. Tris-(8-hydroxyquinoline)

aluminum nanoparticles prepared by vapor condensation. Applied Physics Letters, 2003, 83(2): 347–349
2. Hu J S, Ji H X, Cao A M, Huang Z X, Zhang Y, Wan L J, Xia A D, Yu D P, Meng X M, Lee S T. Facile solution synthesis of hexagonal Alq3 nanorods and their field emission properties. Chemical Communications (Cambridge), 2007, (29): 3083–3085
3. Chiu J J, Kei C C, Perng T P, Wang W S. Organic semiconductor nanowires for field emission. Advanced Materials, 2003, 15(16): 1361–1364
4. Liu H B, Zhao Q, Li Y L, Liu Y, Lu F S, Zhuang J P, Wang S, Jiang L, Zhu D B, Yu D P, Chi L F. Field emission properties of large-area nanowires of organic charge-transfer complexes. Journal of the American Chemical Society, 2005, 127(4): 1120–1121
5. Kastler M, Pisula W, Laquai F, Kumar A, Davies R J, Baluschev S, Garcia-Gutierrez M C, Wasserfallen D, Butt H J, Riekel C, Wegner G, Mullen K. Organization of charge-carrier pathways for organic electronics. Advanced Materials, 2006, 18(17): 2255–2259
6. Cho C P, Yu C Y, Perng T P. Growth of AlQ_3 nanowires directly from amorphous thin film and nanoparticles. Nanotechnology, 2006, 17(21): 5506–5510
7. Xia Y N, Yang P D, Sun Y G, Wu Y Y, Mayers B, Gates B, Yin Y D, Kim F, Yan Y Q. One-dimensional nanostructures: synthesis, characterization, and applications. Advanced Materials, 2003, 15 (5): 353–389
8. Zhang X J, Jie J S, Zhang W F, Zhang C Y, Luo L B, He Z B, Zhang X H, Zhang W J, Lee C S, Lee S T. Photoconductivity of a single small-molecule organic nanowire. Advanced Materials, 2008, 20 (12): 2427–2432
9. Hu J S, Guo Y G, Liang H P, Wan L J, Jiang L. Three-dimensional self-organization of supramolecular self-assembled porphyrin hollow hexagonal nanoprisms. Journal of the American Chemical Society, 2005, 127(48): 17090–17095
10. Zhao Y S, Fu H B, Peng A D, Ma Y, Xiao D B, Yao J N. Low-dimensional nanomaterials based on small organic molecules: preparation and optoelectronic properties. Advanced Materials, 2008, 20(15): 2859–2876
11. Zhang X J, Zhang X H, Zou K, Lee C S, Lee S T. Single-crystal nanoribbons, nanotubes, and nanowires from intramolecular charge-transfer organic molecules. Journal of the American Chemical Society, 2007, 129(12): 3527–3532
12. An B K, Lee D S, Lee J S, Park Y S, Song H S, Park S Y. Strongly fluorescent organogel system comprising fibrillar self-assembly of a trifluoromethyl-based cyanostilbene derivative. Journal of the American Chemical Society, 2004, 126(33): 10232–10233
13. Zhao L Y, Yang W S, Luo Y, Zhai T Y, Zhang G J, Yao J N. Nanotubes from isomeric dibenzoylmethane molecules. Chemistry—A European Journal, 2005, 11(12): 3773–3778
14. Zhao Y S, Xiao D B, Yang W S, Peng A D, Yao J N. 2,4,5-triphenylimidazole nanowires with fluorescence narrowing spectra prepared through the adsorbent-assisted physical vapor deposition method. Chemistry of Materials, 2006, 18(9): 2302–2306
15. Tang C W, VanSlyke S A. Organic electroluminescent diodes. Applied Physics Letters, 1987, 51(12): 913–915
16. Mitchell K, Ibers J A. Rare-earth transition-metal chalcogenides. Chemical Reviews, 2002, 102(6): 1929–1952
17. Xu C Q, Zhang Z C, Ye Q. A novel facile method to metal sulfide (metal = Cd, Ag, Hg) nano-crystallite. Materials Letters, 2004, 58 (11): 1671–1676
18. Wang X H, Shao M W, Shao G, Wang S W. Tris(8-hydroxyquinoline)aluminum nanoribbons: facile solvothermal preparation and photoconductivity studies. Journal of Nanoscience and Nanotechnology, 2009, 9(8): 4709–4714
19. Chen W, Peng Q, Li Y D. Luminescent bis-(8-hydroxyquinoline) cadmium complex nanorods. Crystal Growth & Design, 2008, 8(2): 564–567
20. Pan H C, Liang F P, Mao C J, Zhu J J, Chen H Y. Highly luminescent zinc(II)-bis(8-hydroxyquinoline) complex nanorods: sonochemical synthesis, characterizations, and protein sensing. Journal of Physical Chemistry B, 2007, 111(20): 5767–5772
21. Hesse R. Indexing powder photographs of tetragonal, hexagonal and orthorhombic crystals. Acta Crystallographica, 1948, 1(4): 200–207
22. Lipson H. Indexing powder photographs of orthorhombic crystals. Acta Crystallographica, 1949, 2(1): 43–45
23. Tackett J E, Sawyer D T. Properties and infrared spectra in the potassium bromide region of 8-quinolinol and its metal chelates. Inorganic Chemistry, 1964, 3(5): 692–696
24. Tang Q X, Li H X, Liu Y L, Hu W P. High-performance air-stable n-type transistors with an asymmetrical device configuration based on organic single-crystalline submicrometer/nanometer ribbons. Journal of the American Chemical Society, 2006, 128(45): 14634–14639
25. Li Q H, Wan Q, Liang Y X, Wang T H. Electronic transport through individual ZnO nanowires. Applied Physics Letters, 2004, 84(22): 4556–4558